Performance of the Standardized Precipitation Index Based on the TMPA and CMORPH Precipitation Products for Drought Monitoring in China

Lu, Jing; Jia, Li; Menenti, Massimo; Yan, Yuping; Zheng, Chaolei; Zhou, Jie

DOI
10.1109/JSTARS.2018.2810163

Publication date
2018

Document Version
Final published version

Published in
IEEE Journal of Selected Topics in Applied Earth Observations and Remote Sensing

Performance of the Standardized Precipitation Index Based on the TMPA and CMORPH Precipitation Products for Drought Monitoring in China

Jing Lu, Li Jia, Massimo Menenti, Yuping Yan, Chaolei Zheng, and Jie Zhou

***Abstract*—This paper evaluated the accuracy of multiple satellite-based precipitation products including the tropical rainfall measuring mission multisatellite precipitation analysis (TMPA) (TMPA 3B42RT and TMPA 3B42 version 7) and the Climate Prediction Center MORPHing technique (CMORPH) (CMORPH RAW and CMORPH BLD version 1.0) datasets and investigated the impact of the accuracy and temporal coverage of these data products on the reliability of the standardized precipitation index (SPI) estimates. The satellite-based SPI was compared with the SPI estimate using *in situ* precipitation observations from 2221 meteorological observation sites across China from 1998 to 2014. The SPI values calculated from the products calibrated with rain gauge measurements (TMPA 3B42 and CMORPH BLD) are generally more consistent with the SPI obtained with *in situ* measurements than those obtained using noncalibrated products (TMPA 3B42RT and CMORPH RAW products). The short data record of satellite precipitation data products is not the primary source of large errors in the SPI estimates, suggesting that the SPI estimate using satellite precipitation data products can be applied to drought assessment and monitoring. Satellite-based SPI estimates are more accurate in eastern China than in western China because of larger uncertainties in precipitation retrievals in western China, characterized by arid and semiarid climate conditions and complex landscapes. The satellite-based SPI can capture typical drought events throughout China, with the limitation that it is based on precipitation only and that different durations of antecedent precipitation are only suitable for specific drought conditions.**

***Index Terms*—Drought, precipitation, remote sensing, standardized precipitation index.**

Manuscript received August 22, 2017; revised January 25, 2018; accepted February 13, 2018. Date of publication March 18, 2018; date of current version May 1, 2018.This work was supported in part by the Strategic Priority Research Program of the Chinese Academy of Sciences under Grant XDA19030203, in part by the National Natural Science Foundation of China under Grant 41501405, in part by the Long-Term Projects of the 1000 Talent Plan for High-Level Foreign Experts under Grant WQ20141100224, in part by the Youth Scientist Foundation Project of the State Key Laboratory of Remote Sensing Science under Grant Y4Y00200KZ, and in part by the Drought Meteorological Science Research Foundation under Grant IAM201508. *(Corresponding author: Li Jia.)*

J. Lu is with the State Key Laboratory of Remote Sensing Science, Institute of Remote Sensing and Digital Earth, Chinese Academy of Sciences, Beijing, 100101, China, and also with the Institute of the Arid Meteorology of China Meteorological Administration, Lanzhou, 730020, China (e-mail: lujing@radi.ac.cn).

L. Jia, C. Zheng, and J. Zhou are with the State Key Laboratory of Remote Sensing Science, Institute of Remote Sensing and Digital Earth, Chinese Academy of Sciences, Beijing, 100101, China (e-mail: jiali@radi.ac.cn; zhengcl@radi.ac.cn; zhoujie@radi.ac.cn).

M. Menenti is with the State Key Laboratory of Remote Sensing Science, Institute of Remote Sensing and Digital Earth, Chinese Academy of Sciences, Beijing, 100101, China, and also with the Delft University of Technology, Delft, The Netherlands (e-mail: m.menenti@radi.ac.cn).

Y. Yan is with the National Climate Center, China Meteorological Administration, Beijing, 100081, China (e-mail: yanyp@cma.gov.cn).

Color versions of one or more of the figures in this paper are available online at http://ieeexplore.ieee.org.

Digital Object Identifier 10.1109/JSTARS.2018.2810163

I. Introduction

DROUGHT is one of the most severe natural disasters and can lead to large economic losses and threaten national food security [1], [2]. With the increase in drought extent and severity in the twenty-first century [3], drought monitoring based on satellite data is becoming increasingly useful [4]–[7]. AghaKouchak *et al*. reviewed the progress, challenges, and opportunities of remote sensing-based drought assessment and monitoring and pointed out that the current short data record of available satellite observations is a major limitation on drought monitoring from a climate perspective. In addition, data continuity, unquantified uncertainty, sensor changes, and community acceptability also hinder drought monitoring with satellite data products [8].

The occurrence of a drought is initially caused by the lack of precipitation during a certain period, which triggers the causal chain of agricultural drought, hydrological drought, and socioeconomic drought [9]–[12]. The launches of the Tropical Rainfall Measuring Mission (TRMM) in 1997 and the Global Precipitation Measurement mission in 2014 provide advanced approaches for precipitation observations at both the regional and global scales. However, the high uncertainties and relatively short temporal coverage of satellite-based precipitation datasets for drought monitoring remain outstanding issues.

TRMM multisatellite precipitation analysis (TMPA) data [13] and Climate Prediction Center (CPC) MORPHing technique (CMORPH) data [14] are two well-known satellite-based precipitation data products [15]–[18] that have been used for drought monitoring in many regions worldwide. Sahoo *et al*. evaluated the TMPA 3B42v6, 3B42v7, and 3B42RTv7 products for the assessment of meteorological drought worldwide using the standardized precipitation index (SPI) [19]. The results indicated that TMPA data can provide useful information for drought monitoring, but caution should be taken when using the 3B42RTv7 product for the real-time monitoring of drought conditions due to the lack of corrections based on gauge

observations. Naumann *et al*. analyzed the uncertainties in TMPA data and suggested that relatively short time series of satellite precipitation products can be used for reliable drought monitoring over Africa [20]. Zeng *et al*. assessed the ability of TMPA 3B43v6 data to monitor drought in the Lancang River Basin in China by studying two severe drought events in 2006 and 2009 [21]. The results showed that TMPA 3B43v6 data have the potential to monitor drought in data-scarce regions. Li *et al*. investigated the temporal and spatial variations of dry/wet conditions in the Poyang Lake Basin in China using TMPA 3B42 data, and concluded that the satellite-based SPI exhibited an interannual variability consistent with rain gauge data [22]. Lu *et al*. also used monthly TMPA 3B43v7 data to analyze the characteristics of summer drought in Henan Province in 2004 and concluded that the data did capture the drought event effectively [23].

Most of these studies were based on outdated TMPA data. The most recent, high-quality versions of the datasets (TMPA v7 and CMORPH v1.0 data products) have not yet been widely used. In China, the evaluation of satellite precipitation data for drought monitoring purposes focused on small river basins. In contrast, this study will use recent versions of the TMPA and CMORPH precipitation datasets for drought monitoring at the national scale.

The SPI is a widely used estimator of the severity of a drought [24]–[27] and requires observations of precipitation over an extended and continuous period. It is generally accepted that a minimum data record of 30 years is necessary for SPI calculation [28]. Compared with rain gauge observations, the TMPA and CMORPH data records are relatively short (no more than 20 years). Wu *et al*. investigated the effects of the length of the data record on SPI estimates and demonstrated that the SPI values computed using data records of variable lengths are highly correlated and consistent when the gamma distribution of precipitation over different periods is similar [29]. However, their analysis mainly focused on data records of 30 years or longer. Rhee and Carbone discussed the impact of shorter data records on SPI estimates in the United States, and concluded that short data records, e.g., 10–20 years, generally produced small mean cross-validation absolute errors on SPI [30]. The lengths of the TMPA and CMORPH precipitation data records should be analyzed to determine whether they are sufficient for drought monitoring in China.

The somewhat conflicting evidence summarized above suggests that even short precipitation data records may provide reliable SPI estimates, but this needs to be evaluated region by region. This study will evaluate the TMPA v7 and CMORPH v1.0 precipitation products throughout China using all available rain gauge data. The evaluation method and data are introduced in Sections II and III, respectively. The accuracies of both precipitation data products and the SPI estimates obtained with them are documented by these evaluations, which are given in Sections IV-A–C. The performance of satellite-based SPI estimates in the monitoring of extreme drought events in China is assessed in Section IV-D. Finally, Section V summarizes the conclusions.

TABLE I
LEVELS OF DROUGHT SEVERITY DEFINED BY RANGES OF SPI VALUES

Level	Class	SPI value
D0	No drought	$-0.5 < \text{SPI}$
D1	Light drought	$-1.0 < \text{SPI} \leq -0.5$
D2	Mild drought	$-1.5 < \text{SPI} \leq -1.0$
D3	Severe drought	$-2.0 < \text{SPI} \leq -1.5$
D4	Extreme drought	$\text{SPI} \leq -2.0$

II. METHOD

A. Drought Monitoring Method: The Standardized Precipitation Index

The SPI is widely utilized as a drought monitoring index because it captures drought conditions at different time scales [28], [31]. The SPI is based on the standardized probability of precipitation, so $\text{SPI} = 0$ indicates the median precipitation amount, while $\text{SPI} < 0$ reflects drought, and $\text{SPI} > 0$ implies wet conditions. The determination of a probability density function for precipitation is essential for calculating the SPI and this calculation may be influenced by the length of the data record. The generally accepted gamma probability density function is widely used by numerous agencies, including the National Drought Mitigation Center, the Western Regional Climate Center, and the National Agricultural Decision Support System in the United States. We calculated the SPI using the gamma probability density function and according to the procedure in [32], as detailed in Appendix A.

The levels of drought severity defined by SPI ranges are shown in Table I. These ranges are derived from the "Classification of Meteorological Drought" defined by China National Standardization Management Committee.

To assess the impact of the precipitation record length on the SPI estimates, SPI values obtained with record lengths from 1 to 30 years were evaluated. To separate the impact of the accuracy of the precipitation data products from the impact of the data record, the evaluation was conducted using rain gauge measurements from the 2221 stations with long-term records. The SPI estimates based on a consecutive 30-year precipitation record were considered as references to assess the results obtained using shorter records.

B. Evaluation Method

Multiple metrics were applied to evaluate the quality of both the precipitation data products and SPI estimates. These metrics include the correlation coefficient (R), the root mean square error (RMSE), the mean bias error (MBIAS), the relative bias (RBIAS), and the Nash–Sutcliffe efficiency (NSE), which are expressed as follows:

$$R = \frac{n\sum XY - \sum X \sum Y}{\sqrt{n\sum X^2 - \left(\sum X\right)^2}\sqrt{n\sum Y^2 - \left(\sum Y\right)^2}} \quad (1)$$

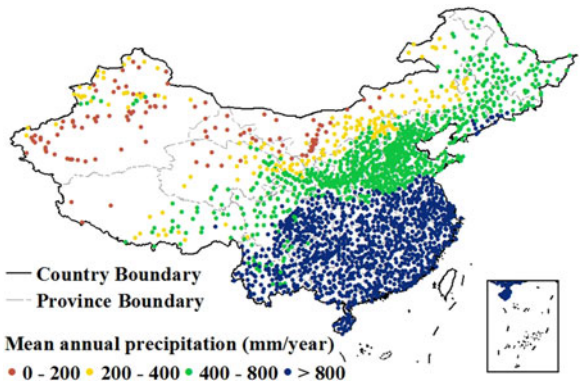

Fig. 1. Distribution of national standard weather stations and their mean annual precipitations. Mean annual precipitations are calculated by the averages of rain gauge measurements from 1985 to 2014.

$$\mathrm{RMSE} = \sqrt{\frac{\sum (X-Y)^2}{n}} \tag{2}$$

$$\mathrm{MBIAS} = \frac{\sum (X-Y)}{n} \tag{3}$$

$$\mathrm{RBIAS} = \frac{\mathrm{MBIAS}}{\bar{Y}} \times 100\% \tag{4}$$

$$\mathrm{NSE} = 1 - \frac{\sum (X-Y)^2}{\sum \left(Y-\bar{Y}\right)^2} \tag{5}$$

where X and Y are the estimates and reference values, respectively. The SPI values calculated using rain gauge measurements are generally considered as references. The larger the values of $|R|$, the lower the RMSE, and the closer to zero MBIAS and RBIAS indicate that estimates are closer to the reference values, thereby reflecting a high reliability of the estimates. The NSE values range from negative infinity (poor skill) to one (perfect skill). An NSE value of 0.4 is considered to be the threshold value for a satisfactory data quality in this study [33], [34].

III. Data

A. Rain Gauge Measurements

Rain gauge measurements were obtained from the "China Daily Ground Climate Dataset v3.0" provided by the China Meteorological Administration (CMA) (http://data.cma.cn). The dataset includes the daily precipitation observations from 2474 national standard weather stations covering the period from 1951 to the present. For precipitation observation, rain gauges have no heated funnel in cold region and no wind shield in windy regions. About 2221 of those stations were ultimately selected because they have data records of 30 consecutive years from 1985 to 2014. In general, there are more stations in the south (east) than in the north (west) of China (see Fig. 1). The mean annual precipitation gradually decreases from the southeast to the northwest in China due to the East Asian monsoon. Arid, semiarid, semihumid, and humid climatic regions of China are distinguished by annual precipitations of 0–200 mm, 200–400 mm, 400–800 mm, and >800 mm, respectively, as shown in Fig. 1.

B. Satellite-Based Precipitation Data

The latest versions of the TMPA (https://disc2.gesdisc.eosdis.nasa.gov/data) and CMORPH (ftp.cpc.ncep.noaa.gov/precip/CMORPH_V1.0) data products were used in this study. The TMPA 3B42RT and CMORPH RAW retrievals were obtained directly from satellite observations that integrate infrared and passive microwave radiance without any further calibration with rain gauge observations. TMPA 3B42 and CMORPH BLD are research products that have been calibrated with rain gauge observations. Approximately 500 gauges over China collected by the Global Precipitation Climatology Center were used in the TMPA 3B42 product, while approximately 200 gauges from the China Global Telecommunication System collected by the CPC were used to generate the CMORPH BLD product [35]. Additional details about the generation of the precipitation data products are provided in [13], [36]–[38]. The TMPA data provide precipitation estimates between 50 °N and 50 °S, while the CMORPH data provides estimates between 60 °N and 60 °S. The TMPA 3B42RT and TMPA 3B42 products both have 3-h interval, while the CMORPH RAW and CMORPH BLD products have daily temporal resolutions. All products cover a period from 1998 to present, with the exception of TMPA 3B42RT, which provides data beginning in 2001. Data from prior to 2014 are used in this study. Monthly and annual values were calculated from hourly or daily precipitation data. All the data have a 0.25° spatial resolution.

IV. Results

A. Preliminary Assessment of Satellite-Based Precipitation

Compared with previous evaluations of satellite precipitation products throughout China [18], [39], [40], this evaluation uses the new versions of the TMPA v7 and CMORPH v1.0 products. The extracted satellite precipitation data are from the grid points including each rain gauge sites and are compared with *in situ* observations. The annual precipitation from the four satellite-based products are rather consistent with the rain gauge measurements, with R values from 0.82 to 0.96 and NSE values from 0.52 to 0.90 (see Fig. 2). The calibrated satellite products (TMPA 3B42 and CMORPH BLD) agreed better consistently with ground observations than the TMPA 3B42RT and CMORPH RAW products, which suggests that the quality of satellite precipitation data can be largely improved by the calibration with rain gauge measurements. Except the uncertainty of satellite retrieval precipitation, the mismatch spatial scale from satellite and ground-based observations is also an important reason for the inconsistent assessment results. The cumulative distribution function (CDF) of NSE based on the evaluation of 2221 rain gauge stations is shown in Fig. 3, and 62% of stations exhibit a satisfactory NSE $>$ 0.4 for the CMORPH BLD product. Approximately 55% of stations exhibit a satisfactory NSE value for the TMPA 3B42 product. Only 10% of stations give NSE $>$ 0.4 for the TMPA 3B42RT product, and fewer than 6% of stations give a satisfactory NSE for the CMORPH RAW product. Overall, the CMORPH BLD product followed

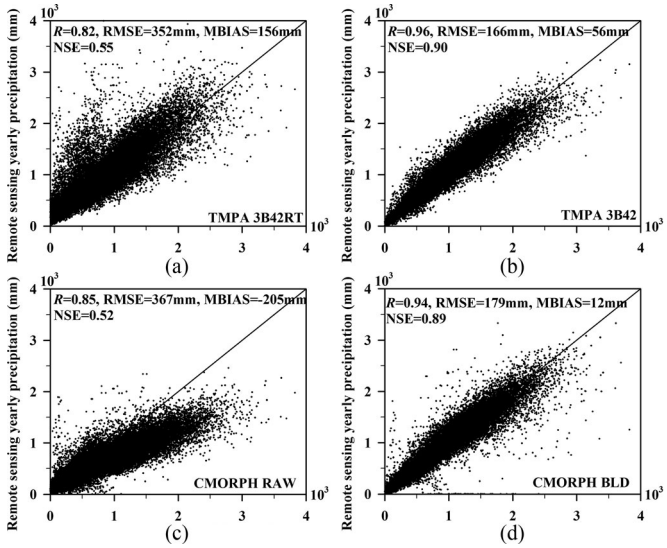

Fig. 2. Comparisons of the annual precipitation values from satellite-based data with rain gauge measurements. (a) TMPA 3B42RT. (b) TMPA 3B42. (c) CMORPH RAW. (d) CMORPH BLD.

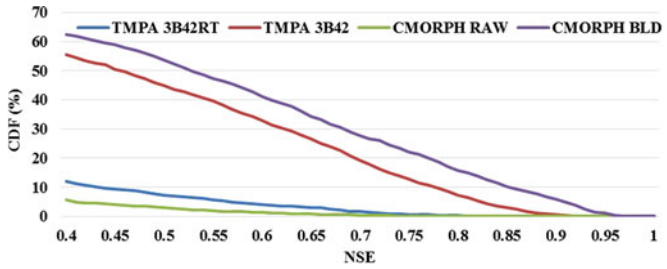

Fig. 3. Cumulative distribution function (CDF) of the Nash–Sutcliffe efficiency (NSE) based on an evaluation of 2221 stations observations.

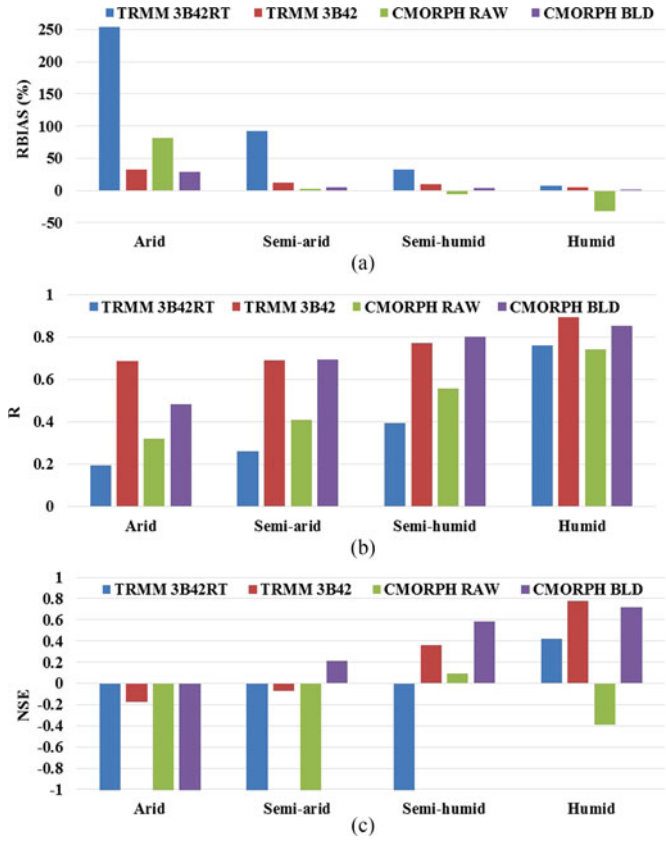

Fig. 4. (a) Relative mean bias (RBIAS). (b) Correction coefficient (R). (c) Nash–Sutcliffe efficiency (NSE) of the four satellite-based precipitation evaluations in four different arid and humid regions.

by TMPA 3B42 exhibits the best agreement with the ground observations of annual precipitation.

It appears that the TMPA 3B42RT product overestimates annual precipitation when smaller than 800 mm [see Fig. 2(a)], while the CMORPH RAW product underestimates precipitation when larger than 800 mm [see Fig. 2(c)]. The same data products were evaluated under arid and humid conditions (see Fig. 4). Overall, the four products slightly overestimate precipitation, with the exception of the slight underestimates in the CMORPH RAW product over humid areas [see Fig. 4(a)]. Similar underestimates in the CMORPH RAW product were reported earlier and are most likely due to the inability of the CMORPH RAW product to effectively capture extremely heavy precipitation in humid and warm regions [41]. The RBIAS is larger than 50% for both the TMPA 3B42RT and CMORPH RAW products and reaches a maximum in arid areas and gradually decreases with increasingly humid conditions [see Fig. 4(a)]. The R values gradually increase from arid to humid regions [see (Fig. 4(b)]. These findings suggest that satellite-based products can more effectively estimate annual precipitation in humid areas than in arid areas. The NSE values in Fig. 4(c) show that the TMPA data are only accurate in humid areas, while the CMORPH BLD data are more accurate in semihumid and humid areas than in arid and semiarid areas. It appears that the TMPA 3B42 and CMORPH BLD products calibrated with rain gauge observations is not sufficient in arid and semiarid areas. As shown in Fig. 1, our study targeted the arid and semiarid areas in western China and the humid and semihumid areas in southern and eastern China. Given the accuracy of the rain gauge observations and the satellite precipitation data products, it becomes challenging to capture the large spatial and temporal variability of precipitation in the arid and semiarid areas of western China. Moreover, it is even more challenging to accurately estimate precipitation in the complex terrain of western China (e.g., the Tibetan Plateau). Insufficient ground-based rainfall observations also limited the calibration of the TMPA 3B42 and CMORPH BLD products [40], [42], [43].

The precipitation over China has a seasonal cycle due to the monsoon. Most of the rainfall generally falls during the summer and a small fraction of annual precipitation occurs in the winter. Monthly precipitation was also evaluated and the results show that the monthly NSE values for the TMPA 3B42 and CMORPH BLD data are nearly constant around 0.8 (see Fig. 5). Relatively large differences can be observed in January, February, November, and December, and the performance of TMPA 3B42 is slightly better than that of CMORPH BLD. The variability of NSE for CMORPH RAW and TMPA 3B42RT is considerable and the NSE values for the CMORPH RAW product are generally larger than those for the TMPA 3B42RT product. Both have better performance from March to October than in other

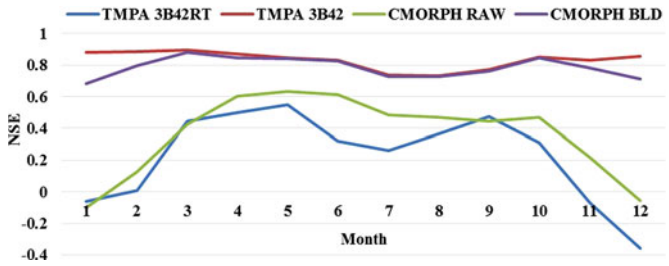

Fig. 5. Nash–Sutcliffe efficiency (NSE) values of the satellite-based monthly precipitation data products compared with rain gauge measurements.

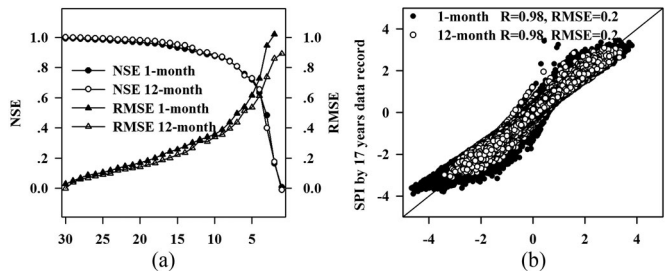

Fig. 6. (a) Nash–Sutcliffe efficiency (NSE) and the root mean square error (RMSE) of SPI values obtained with different data record lengths compared with those based on a consecutive 30-year precipitation record. (b) 1-month and 12-month SPI calculated using 17 years data versus the values based on 30 years of recorded data.

months, which is related to the seasonal distribution of precipitation in China (i.e., more rainfall in summer than in winter). Moreover, these results are consistent with previous conclusions [16], [44]–[46] and imply that satellite observations can capture heavy rainfall better than light rain or winter snow. This finding also partly explains why satellite precipitation data products are more accurate in humid regions, where precipitation is higher throughout the year. The larger precipitation observation error in cold or windy regions also leads to the inconsistency between satellite-based precipitation and rain gauge measurements. The higher NSE values of TMPA 3B42 and CMORPH BLD clearly document the benefit of calibration with rain gauge observations.

B. Consistency of SPI Values Calculated With Different Data Record Lengths

The NSE decreases and the RMSE increases as the data record length decreases. When the length of data records is less than 10 years, the NSE is less than 0.9, and the RMSE is greater than 0.4 [see Fig. 6(a)], which indicates that the larger errors may become unacceptable with shorter data records. The SPI values calculated using a 17-year record from 1998 to 2014 (i.e., the period covered by the satellite precipitation data products) versus those based on the complete 30-year record from 1985 to 2014 are plotted in Fig. 6(b). The results show that RMSE = 0.2 and $R = 0.98$ when using the 17-year data record, i.e., SPI estimates based on a 17-year precipitation data record are rather accurate. Two different durations of the antecedent precipitation, i.e., 1-month and 12-month periods, were also applied to estimate SPI (see Fig. 6). There is no obvious difference in the

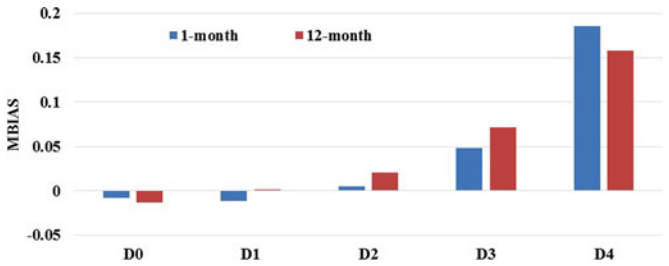

Fig. 7. Mean bias error (MBIAS) of the SPI values resulting from 17-year data records at different drought levels.

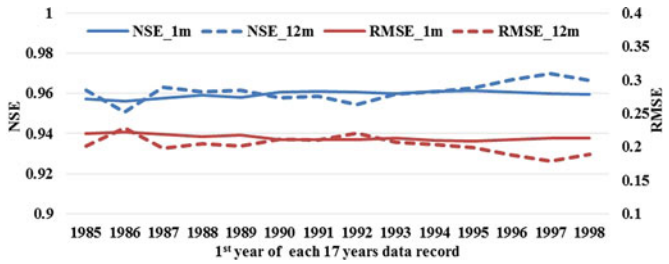

Fig. 8. Comparison of the SPI values from 1998 to 2001 calculated using any consecutive 17-year record within the period of 1985 to 2014 with those using the 30-year record (1m and 12m means respectively the 1-month and 12-month scale for SPI calculation).

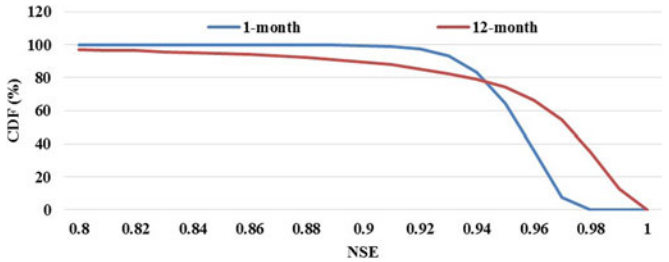

Fig. 9. Cumulative distribution function (CDF) of the Nash–Sutcliffe efficiency (NSE) between 30-years and 17-year record-based SPI comparison for all available rain gauge stations.

results obtained using 1-month or 12-month cumulative precipitation data. The 12-month estimates gave slightly better results than the 1-month estimates, suggesting the longer duration of cumulative precipitation apparently filters out random errors in monthly precipitation [47].

However, MBIAS in the SPI estimates based on the 17-year data record increases with the increasing drought severity (see Fig. 7). Under extreme drought conditions, the SPI is generally overestimated by approximately 0.15, i.e., the SPI based on shorter records slightly underestimates drought severity.

We generated fourteen 17-year data records starting in each year between 1985 and 1998, and all data records include the period 1998 to 2001. These records are used for the evaluation against the SPI estimates based on the 30-year record (see Fig. 8). The NSE and RMSE values fluctuates around 0.96 and 0.2, respectively, indicating that differences in the distribution of precipitation across the 14 realizations of the 17-year data record have a negligible impact on the accuracy of SPI estimates. The CDF analysis shows that the NSE values are larger than 0.8 for all stations (see Fig. 9), i.e., the impact of the length

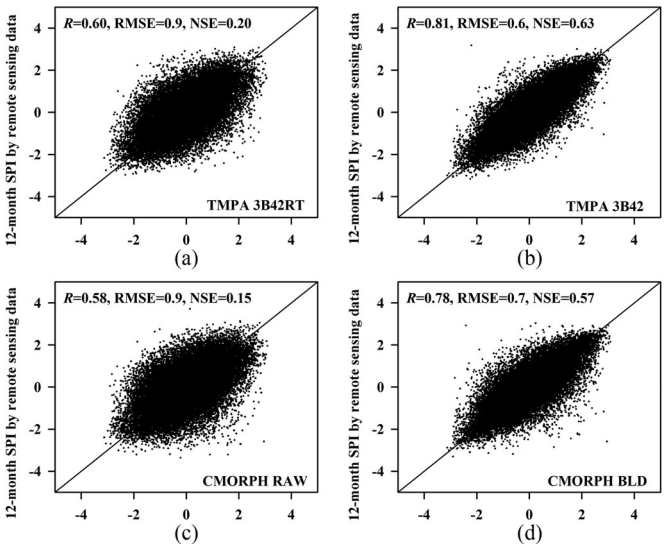

Fig. 10. Comparison of the 12-month SPI calculated using the satellite precipitation data products versus that calculated using the rain gauge measurements, for (a) TMPA 3B42RT, (b) TMPA 3B42, (c) CMORPH RAW, and (d) CMORPH BLD products.

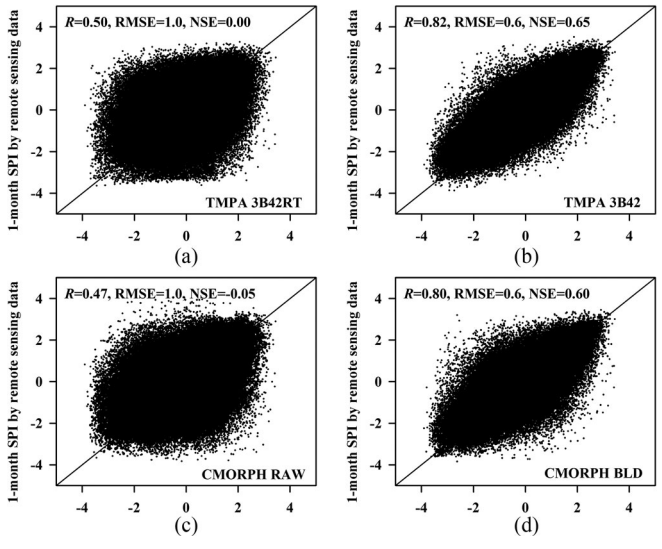

Fig. 11. Same as Fig. 10, but for the 1-month SPI.

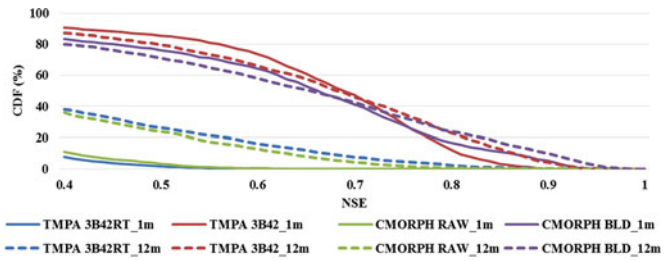

Fig. 12. Cumulative distribution function (CDF) of the Nash–Sutcliffe efficiency (NSE) for the SPI at different time scales.

of the precipitation data record on SPI estimates does not depend on the location of the stations. This result is also consistent with the conclusions of previous studies [29], [30] and suggests that the shorter length of the satellite precipitation data records is not the main source of errors in the SPI estimates.

C. Evaluation of Satellite-Based SPI

The accuracy of the precipitation data products (see Section IV-A) does not necessarily have the same impact on the accuracy of SPI estimates, because the SPI is calculated using the probability of a given amount of precipitation. Accordingly, the four satellite precipitation products are further assessed to analyze their accuracies in the SPI estimates.

Time series of satellite precipitation data were extracted for each station as described in Section IV-A, then SPI was estimated and compared with the estimates obtained from the rain gauge measurements from 1998 to 2014. The MBIAS is almost 0 for all SPI comparisons (Figs. 10 and 11), as expected because of the normalization process applied to estimate SPI. The calibrated data products, TMPA 3B42 and CMORPH BLD, give SPI estimates in good agreement with those based on rain gauge observations with NSE of approximately 0.6, while NSE < 0.4 for the TMPA 3B42RT and CMPRPH RAW products. Likewise, TMPA 3B42 and CMORPH BLD give R of approximately 0.8 and RMSE of $\sim$0.6 [see Figs. 10(b) and (d) and 11(b) and (d)] compared to R of $\sim$0.5 and RMSE of $\sim$1.0 for the TMPA 3B42RT and CMPRPH RAW products [see Figs. 10(a) and (c) and 11(a) and (c)]. This means that drought severity can be assessed with the TMPA 3B42 and CMORPH BLD products, but the estimated severity level may be incorrect. When the TMPA 3B42RT and CMPRPH RAW products are used, the assessed severity level may be off by as much as two levels due to the large RMSE.

The CDF analysis reveals that more than 80% of stations give NSE > 0.4 for the TMPA 3B42 and CMORPH BLD products, regardless of whether a 1-month or 12-month duration is used to determine the antecedent precipitation (see Fig. 12). Only 10% of stations give NSE > 0.4 for the TMPA 3B42RT and CMORPH RAW products at a 1-month duration, while 40% of stations exhibit NSE > 0.4 at a 12-month duration, which as noted earlier filters out random errors on precipitation. It appears that the agreement in satellite versus *in situ* SPI estimates (see Fig. 12) is better than in the precipitation data (see Fig. 3). This confirms that the SPI can mitigate the impact of errors in the satellite retrieval of precipitation.

The spatial variability of NSE value for SPI evaluations is large and clearly related to the magnitude of precipitation [see Figs. 13 and 14 for 1-month and 12-month duration, respectively). The NSE values are generally higher in eastern China than in western China, where the precipitation total is lower and more variable and retrievals are less accurate. This implies that satellite precipitation data products can be used to monitor drought in eastern China under humid conditions, while uncertainties are much larger in the west under arid conditions. This finding agrees with the assessment on the accuracy of the satellite precipitation data products (see Section IV-A) and is consistent with the conclusions of a previous investigation [48]. Accurate precipitation retrievals lead to better drought monitoring based on the SPI. Stations in eastern and southern

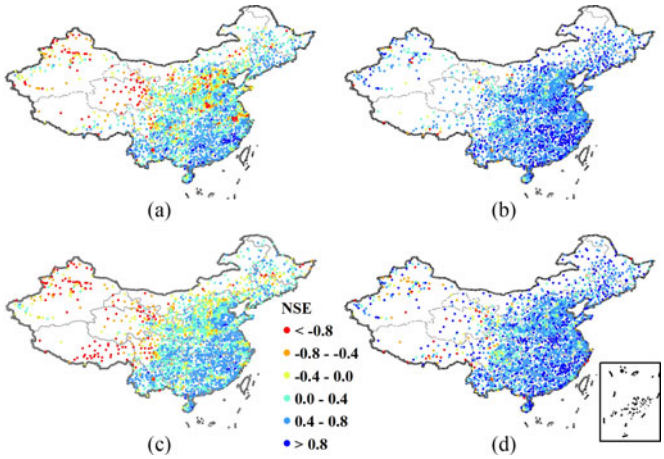

Fig. 13. Spatial distribution of the Nash–Sutcliffe efficiency (NSE) values for the satellite-based 12-month SPI vs. those based on rain gauge measurements, for (a) TMPA 3B42RT, (b) TMPA 3B42, (c) CMORPH RAW, and (d) CMORPH BLD products.

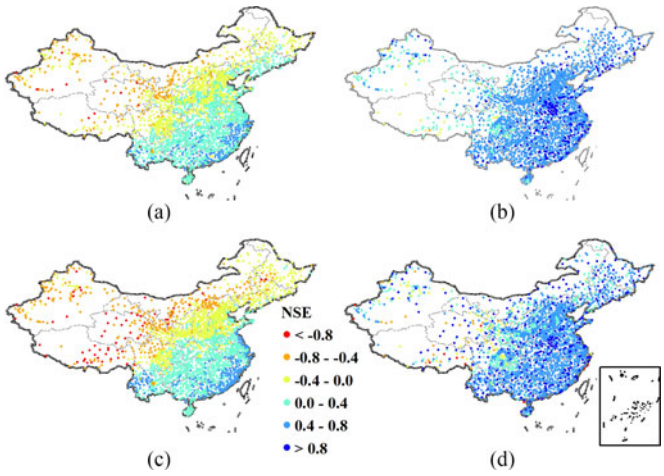

Fig. 14. Same as Fig. 13, but for the 1-month SPI.

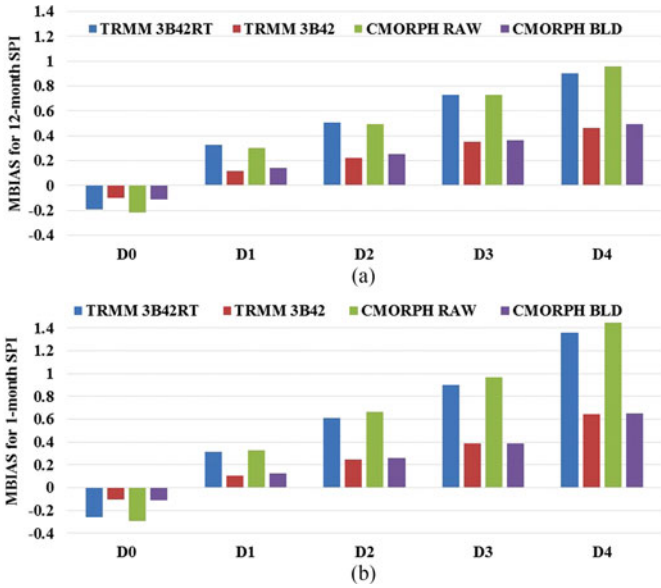

Fig. 15. Mean bias (MBIAS) of satellite-based SPI values at different drought levels for a (a) 12-month scale and (b) 1-month scale.

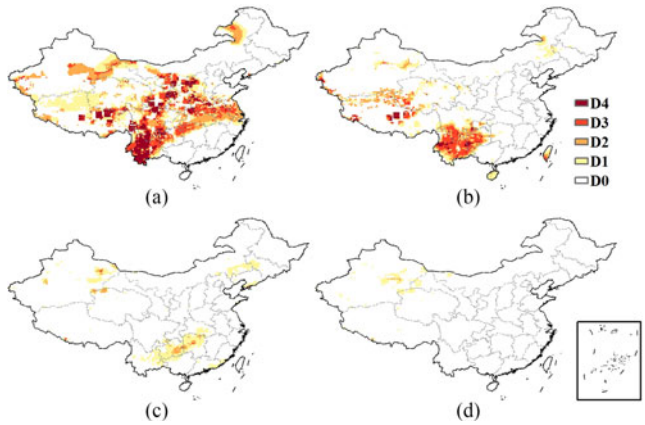

Fig. 16. Drought severity on January 24, 2010 using different durations of antecedent precipitation from the CMORPH BLD products, (a) 1-month, (b) 3-month, (c) 6-month, and (d) 12-month SPI.

China commonly have NSE $>$ 0.4 for the TMPA 3B42RT and CMPRPH RAW products at a 12-month duration relative to a 1-month duration. There is no obvious difference when employing TMPA 3B42 or CMORPH BLD, but more stations give NSE $>$ 0.8 with a 12-month duration than with a 1-month duration, which is consistent with the results in Fig. 12. Clearly, the accuracy of satellite precipitation retrievals in western China under arid and semi-arid climate conditions needs to be improved.

As with the estimates based on rain gauge observations (see Fig. 7), the MBIAS of the satellite-based SPI increases with the increasing drought severity (see Fig. 15). The MBIAS for the 12-month SPI [see Fig. 15(a)] is always lower than that for the 1-month SPI [see Fig. 15(b)] at each drought level. As expected, in all cases, the MBIAS is lower for the TMPA 3B42 and CMORPH BLD data products than for TMPA 3B42RT and CMORPH RAW. The negative MBIAS in the absence of drought conditions suggests that the drought severity level will be overestimated. Conversely, at a higher drought severity level, a positive MBIAS implies that the satellite-based SPI values will be overestimated and drought severity underestimated, especially under extreme drought conditions.

D. Response of Satellite Precipitation Data to Extreme Drought Events

The duration of antecedent precipitation plays a vital role in drought monitoring because it directly influences the SPI values and leads to different classifications of the drought severity level. Although the accuracy of the satellite-based SPI estimates can be improved by increasing the duration of antecedent precipitation, different durations respond to distinct drought types. It is difficult to exactly determine the most appropriate duration for drought monitoring in a specific region, because the occurrence of a drought is related to not only precipitation but also solar radiation, vegetation, soil, and the nature of the irrigation systems.

We assessed the drought severity for two typical drought events (the southwest extreme winter-spring drought in 2010 and the extreme summer drought in Henan Province in 2014) using different durations of antecedent precipitation (1, 3, 6, and 12 months) with the CMORPH BLD products (see Figs. 16

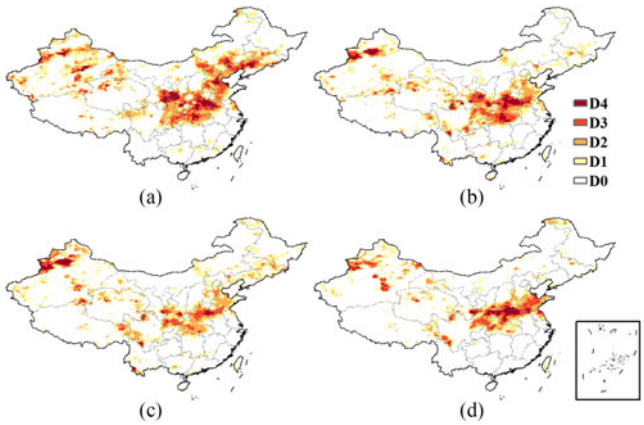

Fig. 17. Same as Fig. 16, but for August 4, 2014.

and 17). The drought assessments from the National Climate Center (NCC) of the CMA (see Appendix B) were used as a reference. The southwest extreme drought occurred in the winter and spring and seriously affected crop growth. The Henan Province extreme drought occurred during the growing season when sufficient water is required for crops. Both drought events led to serious agricultural losses.

For the southwest extreme drought in 2010, the 3-month SPI provides a drought distribution that is most comparable with the CMA assessments. These findings are consistent with the conclusions of a previous study [27], which found that the correlation between the drought severity index and the 3-month SPI was largest. At the same time, some regions in central China also experienced light and mild droughts that could not be detected with the 3-month SPI. This is consistent with the results of Section IV-C, wherein the 3-month SPI led to underestimate the drought severity. The 1-month SPI generally overestimates the drought severity over China during this period because antecedent precipitation is ignored. Moreover, both the 6- and 12-month SPI underestimate the drought severity because precipitation during the longer periods downgrades the assessed drought severity during the actual drought event.

SPI calculations using four different durations did capture the extreme 2014 summer drought event in Henan Province, central China. However, all SPI estimates, with the exception of the 1-month SPI, overestimated droughts in western China and underestimated the drought severity in the south of Northeast China.

Therefore, to monitor droughts of different types, different SPI estimation strategies should be adopted that consider the impacts of the antecedent precipitation, climate regime, hydrological conditions, drought periods, and drought severities. Additional investigations should be conducted in the future on this aspect.

V. Conclusion

Satellite precipitation data products provide an advanced approach for monitoring droughts over large regions. The uncertainties in such data products can influence the reliability of drought assessment. The applicability of four satellite precipitation data products (i.e., TMPA 3B42RT, TMPA 3B42, CMORPH RAW, and CMORPH BLD) to assess and monitor drought throughout China based on the SPI was evaluated. The main conclusions of the study are as follows.

1) The accuracy of remote sensing precipitation retrieval can be improved by calibration with rain gauge measurements. Accuracy is higher in humid and semihumid areas than in arid and semiarid areas, and it is also higher in summer than in winter due to the larger amount of rainfall in summer (in China).
2) SPI calculation is not sensitive to the length of precipitation data record. A 17-year satellite-based precipitation data record is sufficiently long for estimating the SPI and is thus applicable for drought monitoring. The SPI estimated with a shorter data record, however, is increasingly overestimated with increasing drought severity, accordingly leading to the underestimation of drought severity.
3) SPI estimates based on the TMPA 3B42 and CMORPH BLD products are generally in better agreement with those based on rain gauge measurements than those based on the TMPA 3B42RT and CMORPH RAW products. The overall accuracy of the satellite-based 12-month SPI is better than that of the 1-month SPI due to the mitigation of random errors by the longer duration of antecedent precipitation. Satellite-based SPI errors can increase with the increasing drought severity level. Moreover, the accuracy in western China is poorer than in eastern China because of the arid and semi-arid climate conditions.
4) The calibrated precipitation retrievals can generally capture drought events throughout China. However, it is difficult to precisely determine the duration of antecedent precipitation required for SPI estimates for each drought type, especially in western China.

Droughts are complex phenomena and different applications adopt different definitions of droughts. TMPA 3B42 and CMORPH BLD data are accurate, but they depend on rain gauge measurements. Additionally, the relatively low monthly update frequency may be insufficient for the quasi-real-time monitoring of droughts and associated early warning. The TMPA 3B42RT and CMORPH RAW products provide hourly data, but the accuracy is poor and requires further improvement. Therefore, future investigations must be conducted to clarify and reduce the uncertainties in satellite precipitation products for drought monitoring, especially for complex landscapes and arid and semiarid climate conditions.

Appendix

A. Procedure for SPI Calculation: First, provided that the precipitation during a period is x, and its probability density function assuming a gamma distribution is as follows:

$$g(x) = \frac{1}{\beta^{\alpha}\Gamma(\alpha)} x^{\alpha-1} e^{-\frac{x}{\beta}} \quad (x > 0)$$

where α is the shape parameter, β is the scale parameter, and $\Gamma(\alpha)$ is the gamma function. α and β can be estimated with the

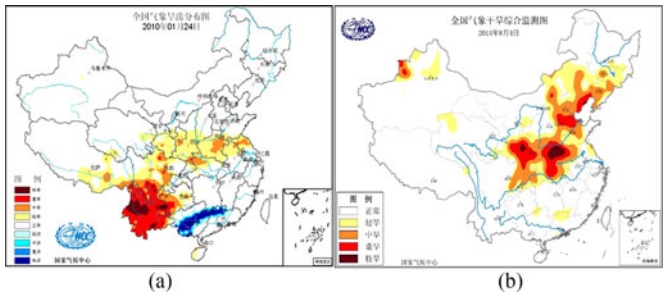

Fig. 18. Drought assessments by the National Climate Center (NCC) of the China Meteorological Administration (CMA) on (a) January 24, 2010, and (b) August 4, 2014.

maximum likelihood method as follows:

$$\hat{\alpha} = \frac{1 + \sqrt{1 + 4A/3}}{4A}$$

$$\hat{\beta} = \frac{\bar{x}}{\hat{\alpha}}$$

where $A = \ln(\bar{x}) - \frac{\sum \ln(x)}{n}$, and n is the length of the time series.

Second, after determining the parameters of the probability density function, the cumulative probability can be calculated as follows:

$$G(x) = \int_0^x g(x)\,dx = \frac{1}{\Gamma(\hat{\alpha})} \int_0^x t^{\hat{\alpha}-1} e^{-1} dt$$

with $t = x/\hat{\beta}$.

The gamma function is not valid when $x = 0$, but the actual precipitation can be 0. Therefore, the cumulative probability is expressed differently as follows:

$$H(x) = q + (1 - q)\,G(x)$$

where q is the probability of zero precipitation and is equal to m/n, where m is the number of days without precipitation in a given time series.

Finally, the cumulative probability $H(x)$ can be transformed into the standard normal distribution function using the following equation:

$$\mathrm{SPI} = P\left(t - \frac{c_0 + c_1 t + c_2 t^2}{1 + d_1 t + d_2 t^2 + d_2 t^2}\right).$$

If $H(x) \le 0.5$, then $P = -1$ and $t = \sqrt{\ln[\frac{1}{H(x)^2}]}$. If $H(x) > 0.5$, then $\mathrm{P} = 1$ and $t = \sqrt{\ln\{\frac{1}{[1-H(x)]^2}\}}$. In addition, $c_0 = 2.515517$; $c_1 = 0.802853$; $c_2 = 0.010328$; $d_1 = 1.432788$; $d_2 = 0.189269$; and $d_3 = 0.001308$. These constant coefficients are derived from the study of Edwards (1997).

B. Drought Events: Drought assessments provided by the NCC of the CMA on January 24, 2010 and August 4, 2014 are shown in Fig. 18. The drought monitoring index of the CMA is based on a relative humidity index that includes evapotranspiration and precipitation from ground-based measurements (http://cmdp.ncc.cma.gov.cn/download/Monitoring/Drought).

REFERENCES

[1] H. C. J. Godfray *et al.*, "Food security: The challenge of feeding 9 billion people," *Science*, vol. 327, pp. 812–818, 2010.

[2] D. A. Wilhite, *Drought and Water Crises: Science, Technology, and Management Issues*. Boca Raton, FL, USA: CRC Press, 2005.

[3] A. Dai, "Increasing drought under global warming in observations and models," *Nature Climate Change*, vol. 3, pp. 52–58, 2012.

[4] M. C. Anderson and W. P. Kustas, "Mapping evapotranspiration and drought at local to continental scales using thermal remote sensing," in *Proc. IEEE Int. Geosci. Remote Sens. Symp.*, 2008, pp. IV-121–IV-123.

[5] L. Damberg and A. AghaKouchak, "Global trends and patterns of drought from space," *Theoretical Appl. Climatol.*, vol. 117, pp. 441–448, 2014.

[6] A. Karnieli *et al.*, "Use of NDVI and land surface temperature for drought assessment: Merits and limitations," *J. Climate*, vol. 23, pp. 618–633, 2010.

[7] L. Wang and J. J. Qu, "Satellite remote sensing applications for surface soil moisture monitoring: A review," *Frontiers Earth Sci. China*, vol. 3, pp. 237–247, 2009.

[8] A. AghaKouchak *et al.*, "Remote sensing of drought: Progress, challenges and opportunities," *Rev. Geophys.*, vol. 53, pp. 452–480, 2015.

[9] L. Jia, G. Hu, J. Zhou, and M. Menenti, "Assessing the sensitivity of two new indicators of vegetation response to water availability for drought monitoring," *Proc. SPIE*, vol. 8524, 2012, Art. no. 85241A.

[10] D. Long *et al.*, "Drought and flood monitoring for a large karst plateau in Southwest China using extended GRACE data," *Remote Sens. Environ.*, vol. 155, pp. 145–160, 2014.

[11] J. Maybank *et al.*, "Drought as a natural disaster," *Atmosphere-Ocean*, vol. 33, pp. 195–222, 1995.

[12] A. K. Mishra and V. P. Singh, "A review of drought concepts," *J. Hydrol.*, vol. 391, pp. 202–216, 2010.

[13] G. Huffman *et al.*, "The TRMM multi-satellite rainfall analysis: Quasi-global, multi-year, combinedsensor rainfall estimates at fine scale," *J. Hydrometeorol.*, vol. 8, pp. 38–55, 2007.

[14] R. J. Joyce, J. E. Janowiak, P. A. Arkin, and P. Xie, "CMORPH: A method that produces global precipitation estimates from passive microwave and infrared data at high spatial and temporal resolution," *J. Hydrometeorol.*, vol. 5, pp. 487–503, 2004.

[15] T. Kubota, T. Ushio, S. Shige, S. Kida, M. Kachi, and K. I. Okamoto, "Verification of high-resolution satellite-based rainfall estimates around Japan Using a Gauge-Calibrated ground-radar dataset," *J. Meteorological Soc. Jpn.*, vol. 87A, pp. 203–222, 2009.

[16] B. Peng, J. Shi, W. Ni-Meister, T. Zhao, and D. Ji, "Evaluation of TRMM Multisatellite Precipitation Analysis (TMPA) products and their potential hydrological application at an arid and semiarid Basin in China," *IEEE J. Sel. Topics Appl. Earth Observ. Remote Sens.*, vol. 7, no. 9, pp. 3915–3930, Sep. 2014.

[17] M. R. P. Sapiano and P. A. Arkin, "An intercomparison and validation of high-resolution satellite precipitation estimates with 3-hourly gauge data," *J. Hydrometeorol.*, vol. 10, pp. 149–166, 2009.

[18] Y. Shen, A. Xiong, Y. Wang, and P. Xie, "Performance of high-resolution satellite precipitation products over China," *J. Geophys. Res., Atmospheres*, vol. 115, pp. 1984–2012, 2010.

[19] A. K. Sahoo, J. Sheffield, M. Pan, and E. F. Wood, "Evaluation of the tropical rainfall measuring mission multi-satellite precipitation analysis (TMPA) for assessment of large-scale meteorological drought," *Remote Sens. Environ.*, vol. 159, pp. 181–193, 2015.

[20] G. Naumann, P. Barbosa, H. Carrao, A. Singleton, and J. Vogt, "Monitoring drought conditions and their uncertainties in Africa using TRMM data," *J. Appl. Meteorol. Climatol.*, vol. 51, pp. 1867–1874, 2012.

[21] H. Zeng, L. Li, and J. Li, "The evaluation of TRMM Multisatellite Precipitation Analysis (TMPA) in drought monitoring in the Lancang River Basin," *J. Geographical Sci.*, vol. 22, pp. 273–282, 2012.

[22] X. Li, Q. Zhang, and X. Ye, "Dry/wet conditions monitoring based on TRMM rainfall data and its reliability validation over Poyang Lake basin, China," *Water*, vol. 5, pp. 1848–1864, 2013.

[23] J. Lu, L. Jia, and J. Zhou, "Characterization of 2014 summer drought over Henan province using remotely sensed data," in *Proc. Int. Conf. Intell. Earth Observing Appl.*, 2015, pp. 980812-1–980812-9.

[24] M. Alamgir, S. Shahid, M. K. Hazarika, S. Nashrrullah, S. B. Harun, and S. Shamsudin, "Analysis of meteorological drought pattern during different climatic and cropping seasons in Bangladesh," *J. Amer. Water Resources Assoc.*, vol. 51, pp. 794–806, 2015.

[25] J. Keyantash and J. A. Dracup, "The quantification of drought: An evaluation of drought indices," *Bull. Amer. Meteorological Soc.*, vol. 83, pp. 1167–1180, 2002.

[26] W. Wang, Y. Zhu, R. Xu, and J. Liu, "Drought severity change in China during 1961–2012 indicated by SPI and SPEI," *Natural Hazards*, vol. 75, pp. 2437–2451, 2015.
[27] X. Q. Zhang and Y. Yamaguchi, "Characterization and evaluation of MODIS-derived Drought Severity Index (DSI) for monitoring the 2009/2010 drought over southwestern China," *Natural Hazards*, vol. 74, pp. 2129–2145, Dec. 2014.
[28] T. B. McKee, N. J. Doesken, and J. Kleist, "The relationship of drought frequency and duration to time scales," in *Proc. 8th Conf. Appl. Climatol.*, Anaheim, CA, USA, 1993, pp. 179–184.
[29] H. Wu, M. J. Hayes, D. A. Wilhite, and M. D. Svoboda, "The effect of the length of record on the standardized precipitation index calculation," *Int. J. Climatol.*, vol. 25, pp. 505–520, 2005.
[30] J. Rhee and G. J. Carbone, "Estimating drought conditions for regions with limited precipitation data," *J. Appl. Meteorol. Climatol.*, vol. 50, pp. 548–559, 2011.
[31] M. Rouault and Y. Richard, "Intensity and spatial extension of drought in South Africa at different time scales," *Water SA*, vol. 29, pp. 489–500, 2003.
[32] D. C. Edwards, "Characteristics of 20th century drought in the United States at multiple time scales," Washington, DC, USA: Storming Media, 1997.
[33] Y. Xia *et al.*, "Continental-scale water and energy flux analysis and validation for the North American land data assimilation system project phase 2 (NLDAS-2): 2. Intercomparison and application of model products," *J. Geophys. Res., Atmospheres*, vol. 117, 2012, Art. no. D03109.
[34] Y. Xia *et al.*, "Application of USDM statistics in NLDAS-2: Optimal blended NLDAS drought index over the continental United States," *J. Geophys. Res., Atmospheres*, vol. 119, pp. 2947–2965, 2014.
[35] Y. Shen and A. Xiong, "Validation and comparison of a new gauge-based precipitation analysis over mainland China," *Int. J. Climatol.*, vol. 36, pp. 252–265, 2016.
[36] R. J. Joyce, P. Xie, Y. Yarosh, J. E. Janowiak, and P. A. Arkin, "CMORPH: A "morphing" approach for high resolution precipitation product generation," in *Satellite Rainfall Applications for Surface Hydrology*, New York, NY, USA: Springer, 2010, pp. 23–37.
[37] P. Xie and A. Y. Xiong, "A conceptual model for constructing high-resolution gauge-satellite merged precipitation analyses," *J. Geophys. Res., Atmospheres*, vol. 116, pp. 1984–2012, 2011.
[38] S. Wang *et al.*, "Evaluation of remotely sensed precipitation and its performance for streamflow simulations in Basins of the Southeast Tibetan Plateau," *J. Hydrometeorol.*, vol. 16, pp. 2577–2594, 2015.
[39] L. Cheng, R. Shen, C. Shi, L. Bai, and Y. Yang, "Evaluation and verification of CMORPH and TRMM 3B42 precipitation estimation products," *Meteorological Monthly*, vol. 40, no. 11, pp. 1372–1379, 2014.
[40] Y. Qin, Z. Chen, Y. Shen, S. Zhang, and R. Shi, "Evaluation of satellite rainfall estimates over the Chinese Mainland," *Remote Sens.*, vol. 6, pp. 11649–11672, 2014.
[41] J. L. A. Khandu and E. Forootan, "An evaluation of high-resolution gridded precipitation products over Bhutan (1998-2012)," *Int. J. Climatol.*, vol. 36, pp. 1067–1087, 2015.
[42] T. Dinku, S. Connor, and P. Ceccato, "Comparison of CMORPH and TRMM-3B42 over Mountainous Regions of Africa and South America," in *Satellite Rainfall Applications for Surface Hydrology*, M. Gebremichael and F. Hossain, Eds. Dordrecht, The Netherlands: Springer, 2010, pp. 193–204.
[43] Y. C. Gao and M. F. Liu, "Evaluation of high-resolution satellite precipitation products using rain gauge observations over the Tibetan Plateau," *Hydrol. Earth Syst. Sci.*, vol. 17, pp. 837–849, 2013.
[44] A. AghaKouchak, A. Mehran, H. Norouzi, and A. Behrangi, "Systematic and random error components in satellite precipitation data sets," *Geophys. Res. Lett.*, vol. 39, 2012, Art. no. L09406.
[45] Y. Yang and Y. Luo, "Evaluating the performance of remote sensing precipitation products CMORPH, PERSIANN, and TMPA, in the arid region of northwest China," *Theoretical Appl. Climatol.*, vol. 118, pp. 429–445, 2014.
[46] F. Chen and X. Li, "Evaluation of IMERG and TRMM 3B43 monthly precipitation products over mainland China," *Remote Sens.*, vol. 8, no. 472, pp. 1–18, 2016.
[47] J. Liu, Z. Duan, J. Jiang, and A. X. Zhu, "Evaluation of three satellite precipitation products TRMM 3B42, CMORPH, and PERSIANN over a subtropical watershed in China," *Adv. Meteorol.*, vol. 2015, pp. 1–13, 2015.
[48] Q. Yang, M. Li, Z. Zheng, and Z. Ma, "Regional applicability of seven meteorological drought indices in China," *Sci. China Earth Sci.*, vol. 60, pp. 745–760, 2017.

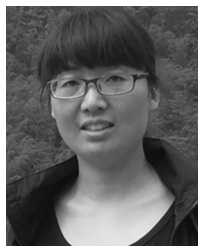

Jing Lu received the Ph.D. degree in geographic information system from the Institute of Geographic Sciences and Nature Recourses Research, Chinese Academy of Science, Beijing, China, in 2014.

She is currently an Assistant Researcher with the Institute of Remote Sensing and Digital Earth, Chinese Academy of Science. Her research interests include remote sensing-based evapotranspiration estimation, drought monitoring, water resource evaluation, and global climate change.

Li Jia received the B.S. degree in dynamic meteorology from the Beijing College of Meteorology, Beijing, China, in 1988, the M.Sc. degree in atmospheric physics from Chinese Academy of Sciences in China, Beijing, in 1997, and the Ph.D. degree in environmental science from Wageningen University, Wageningen, The Netherlands, in 2004.

She is a Professor with the State Key Laboratory of Remote Sensing Science, the Institute of Remote Sensing and Digital Earth, Chinese Academy of Sciences. Her research interests include the study of earth observation and its applications in hydrometeorology, water resource, agriculture, and climate change.

Massimo Menenti received the Ph.D. degree in environmental sciences from the University of Wageningen, Wageningen, The Netherlands, in 1984.

He is currently a foreign expert with the Institute of Remote Sensing and Digital Earth, Chinese Academy of Science, Beijing, China. His research interests include earth observations and the global terrestrial water cycle, including the retrieval of land surface parameters from remote sensing, land surface processes (specifically on heat and water exchanges between the land and atmosphere), time-series analysis of satellite remote sensing observations, and the application of remote sensing in hydrology, agriculture, water resources, crop yields, and climate models.

Yuping Yan received the Ph.D. degree in atmospheric science from the Cold and Arid Regions Environmental and Engineering Research Institute, Chinese Academy of Sciences, Lanzhou, China, in 1999.

She is an Associate Professor with the National Climate Center, China Meteorological Administration, Beijing, China. She had her postdoc fellowship with the climate change institute, Maine University, USA, from 2000 to 2003. She is currently the Director of Operation, Science and Technology Department of National Climate Center. Her research interests include climate change and climate impact assessment.

Chaolei Zheng received the Ph.D. degree in environment energy system from Shizuoka University, Shizuoka, Japan, in 2013.

He is currently an Assistant Researcher with the Institute of Remote Sensing and Digital Earth, Chinese Academy of Science, Beijing, China. His research interests include earth observations of the water cycle, climate change, ecohydrology, and remote sensing.

Jie Zhou received the Ph.D. degree in cartographic and geographic information system from the Institute of Remote Sensing and Digital Earth, Chinese Academy of Science, Beijing, China, in 2016. He is currently working toward another Ph.D. degree in optical and laser remote sensing at the Delft University of Technology, Delft, The Netherlands.

He is an Assistant Researcher with the Institute of Remote Sensing and Digital Earth, Chinese Academy of Science. He was a Visiting Scholar with the Delft University of Technology. His research interests include the time-series analysis of remote sensing data, drought monitoring using earth observations, and application system development.